Surface & Coatings Technology 206 (2011) 250–256

Contents lists available at ScienceDirect

Surface & Coatings Technology

journal homepage: www.elsevier.com/locate/surfcoat

Chemical, physical and morphological characterization of ZnNi films electrodeposited on 1010 steel substrate from acid baths containing polyalcohol

E.M. de Oliveira, I.A. Carlos *

Departamento de Química, Universidade Federal de São Carlos, CP 676, 13565–905, São Carlos-SP, Brazil

ARTICLE INFO

Article history:
Received 17 December 2010
Accepted in revised form 30 June 2011
Available online 8 July 2011

Keywords:
Electrodeposited ZnNi
Sorbitol–boric or mannitol–boric complex
Glycerol
Corrosion

ABSTRACT

ZnNi alloy electrodeposition on a 1010 steel electrode in boric-acid baths containing sorbitol, mannitol or glycerol was investigated by cyclic voltammetry. Electrodeposits obtained galvanostatically were characterized by SEM, EDS and XRD. It was found that in baths containing sorbitol or mannitol, the deposition current density (j_d) was reduced, but in none of the baths was the initial deposition potential affected. SEM images of deposits revealed that the boric-sorbitol and boric-mannitol complexes refine the grain, even at high j_d. XRD patterns of the ZnNi deposits produced at $j_d = 50$ mA cm^{-2}, in ZnNi1 bath and in ZnNi1 bath contained sorbitol or mannitol, indicated that the films were formed mainly of Zn and γ^1 phases. To ZnNi2 baths contained glycerol the films were formed of γ and γ^1 phases. The Ni content in the deposits produced in the bath without polyalcohol or containing glycerol increased from ~5 to 19 wt.% with increasing j_d. With sorbitol or mannitol, there was a smaller rise from ~7 to 10 wt.% Ni. Thus, ZnNi deposits providing sacrificial protection can be obtained in baths with or without polyalcohol. The linear polarization method showed that ZnNi alloy deposited from baths contained polyalcohol have greate R_p.

1. Introduction

ZnNi alloys have been developed with the aim of improving the corrosion resistance of Zn deposited on steel, since Zn coatings have the disadvantage of rapid dissolution [1–3]. ZnNi alloys are good inhibitors of hydrogen permeation on metal substrates [4,5] and adhere well to the substrate [6]. Thus, they are widely employed in the automotive and aerospace industries [1]. ZnNi alloys are also utilized for catalytic purposes, porous Ni electrodes, which have to have a large active surface with a high Ni content. This electrode is used for its small hydrogen and oxygen overpotentials [7,8].

ZnNi deposition baths described in the literature have ammonium chloride as a component, although nowadays there is a strong tendency to replace this with another electrolyte, owing to the difficulty of removing the nickel from the waste electrolyte [9]. Thus, we have investigated the addition of boric acid and polyalcohols such as sorbitol, mannitol or glycerol [10,11] in place of ammonium chloride. In these preliminary works, Pt was used as substrate as it is inert in acid media.

In the previous studies [10,11], it was shown that polyalcohols have various effects on the composition and morphology of ZnNi deposits. Sorbitol or mannitol led to the formation of more compact deposits with finer grain than baths with glycerol or without polyalcohol. Also, sorbitol or mannitol led to the formation of alloys with a narrow range of Ni contents, from ~6 wt.% to ~10 wt.%, while baths containing glycerol or without polyalcohol formed deposits with varying Ni contents, from ~6 wt.% to ~20 wt.%, as the deposition potential became more negative.

In this paper, the effects of adding sorbitol, mannitol or glycerol to boric-acid based ZnNi alloy electrodeposition baths were studied, with 1010 steel as substrate. Voltammetric and galvanostatic electrochemical tests were performed and the morphology, composition and phase composition of the ZnNi deposits were respectively analyzed by scanning electron microscopy (SEM), energy dispersive X-ray spectroscopy (EDS) and X-ray diffraction spectroscopy (XRD).

2. Experimental details

All experiments were carried out at room temperature (25 °C), in a 50 mL glass single-compartment cell. A 1010 steel disk (0.50 cm^2), a platinum plate (~2 cm^2) and a calomel electrode (1.0 M KCl) were employed as working, auxiliary and reference electrodes, respectively. The AISI 1010 steel, from CSN Co. (Brazil), contained 0.04% P, 0.08% C, 0.3% Mn and 0.05% S. Immediately before each experiment, the 1010 steel electrode was ground with 600 emery paper and rinsed with deionized water. The electrodeposition baths of ZnNi alloy contained various concentrations of sorbitol ($C_6H_{14}O_6$), mannitol ($C_6H_{14}O_6$) or glycerol ($C_3H_8O_3$) (Table 1). The pH of the freshly prepared ZnNi bath without polyalcohol or with glycerol was initially ~4.0. However, it was found that after a few deposition voltammetric cycles, the pH of these baths decreased to ~3.0 and after pH 3.0, the pH values of the deposition baths decreased slowly, since pH is a logarithmic function of H_3O^+

* Corresponding author. Tel.: +55 16 3351 8067.
E-mail address: diac@ufscar.br (I.A. Carlos).

0257-8972
doi:10.1016/j.surfcoat.2011.06.061

Table 1
Compositions and pH of bath.

Baths	~pH	Baths	~pH
ZnNi1[a]	3.0	ZnNi1 + 0.26 M glycerol	3.0
ZnNi1 + 0.26 M sorbitol	2.7	ZnNi1 + 0.39 M glycerol	3.0
ZnNi1 + 0.39 M sorbitol	2.6	ZnNi2 + 0.52 M glycerol	3.0
ZnNi2[b] + 0.52 M sorbitol	2.5		
ZnNi1 + 0.26 M mannitol	2.7		
ZnNi1 + 0.39 M mannitol	2.6		
ZnNi2 + 0.52 M mannitol	2.5		

[a] ZnNi1 = 0.55 M $ZnSO_4$ + 0.33 M $NiCl_2$ + 0.22 M $NiSO_4$ + 0.13 M H_3BO_3.
[b] ZnNi2 = 0.55 M $ZnSO_4$ + 0.33 M $NiCl_2$ + 0.22 M $NiSO_4$ + 0.26 M H_3BO_3.

concentration. Thus, as bigger the H_3O^+ concentration in the bath smaller will be the variation in pH values. This fact is known as pseudo buffering effect. Therefore, the pH of the fresh ZnNi bath without polyalcohol or with glycerol (ZnNi1, Table 1), was preadjusted to ~3.0 with H_2SO_4. The fall in the pH from 4.0 to 3.0 was probably due to oxidation of the water at the anode during electrodeposition. The plating baths containing sorbitol or mannitol had an initial pH of 2.80 (0.26 M), 2.60 (0.39 M) and 2.50 (0.52 M). The pH was measured with a Micronal B474 pH meter. Potentiodynamic and galvanostatic curves were recorded with a GAMRY PCI-4 750 mA Potentiostat/Galvanostat. SEM images and EDS measurements were recorded with a Philips FEG XL 30 electron microscope. XRD patterns of the ZnNi deposit surface were produced with Cu Kα radiation (1.5406 Å), using a Rigaku Rotaflex RU200B goniometer, in 2 θ scanning mode (fixed θ = 2°). The parameters used to assess corrosion resistance were measured with a PAR 173 Potentiostatic and galvanostatic electrochemical interface. The linear polarization method [12], at 0.5 mV s^{-1}, was employed and the polarization resistance (R_p) was measured. An aerated solution of 1.0 M Na_2SO_4, pH ~5.0 was used as a corrosive solution. To begin the measurements, the sample was introduced into the electrochemical cell and was allowed to reach equilibrium, which usually took around 10 min. The ZnNi electrodeposits were obtained at current densities (j_d) of 25 and 50 mA cm^{-2} and a deposition charge density (q_d) of 12.21 C cm^{-2} (thickness ~5 μm, obtained by theoretical calculation) and the Zn electrodeposits at 50 mA cm^{-2}, with the same q_d.

3. Results and discussion

3.1. Potentiodynamic and galvanostatic studies of the ZnNi alloy deposition process

Fig. 1a–c shows voltammetric curves of ZnNi deposition, from plating baths of ZnNi1 or ZnNi2 with various sorbitol, mannitol and glycerol concentrations (Table 1), on to a 1010 steel substrate. To facilitate analysis of the voltammograms, they have been divided into regions I and II, where region I corresponds to the potentials before bulk deposition of ZnNi alloy and region II to bulk deposition. It can be seen in Fig. 1a and b that baths containing sorbitol and mannitol produced virtually identical potentiodynamic deposition curves, while in baths containing glycerol (Fig. 1c), the curves were quite different. The similarity in profile of the sorbitol and mannitol baths was probably due to their being isomers, so that in solutions of boric acid they form boric–polyalcohol complexes [13–15] of very similar structure. Having only 3 carbons, glycerol is not an isomer of the 6-carbon polyalcohols, sorbitol and mannitol, and also it does not form a complex with boric acid, owing to the solution pH of 3.0 [10,16].

The initial deposition potential (E_{id}) of the ZnNi alloy obtained from baths studied here shifted between −1.080 V and −1.100 V. However, it was not possible to assert that there was a difference in E_{di} of ZnNi alloy, obtained from various baths, because there is the error of 5 mV associated with the reference electrode. Also, it was observed that the E_{di} shifted in 10 mV in the same bath.

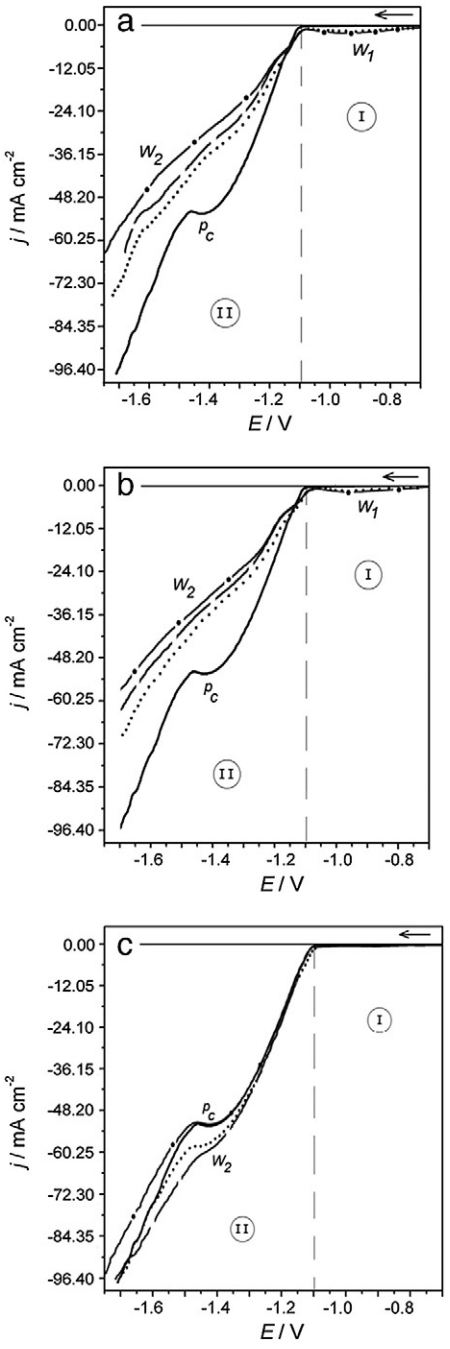

Fig. 1. (a)–(c). Voltammetric curves of ZnNi alloy deposition from electrolytic solutions with various polyalcohol concentrations: a) sorbitol, b) mannitol and c) glycerol, where (—) = ZnNi1, without polyalcohol; (• • •) = ZnNi1 + 0.26 M polyalcohol; (— —) = ZnNi1 + 0.39 M polyalcohol and (— • —) = ZnNi2 + 0.52 M polyalcohol, (see Table 1); υ = 10 mV s^{-1}.

Previous studies on the electrodeposition of ZnNi alloy on a Pt substrate from baths containing sorbitol or glycerol [10], or mannitol [11] showed E_{id} ~ −1.15 V, in all baths. As the previous and the present research were done under the same conditions (the same bath concentrations, electrochemical cell, reference and auxiliary electrode, and potentiodynamic technique), the difference of 50 mV in the E_{id} may be attributed to not only the difference in the work functions of steel (ϕ = 4.5–4.8 eV) and Pt (ϕ = 5.65–5.70 eV) [17], but also to the possible differences in the adsorption of BSC or BMC on steel and Pt substrates in the initial moments of reduction process.

Fig. 1a–c, region I, shows that in the presence of the boric–sorbitol (BSC) or boric–mannitol (BMC) complexes a cathodic wave w_1 was

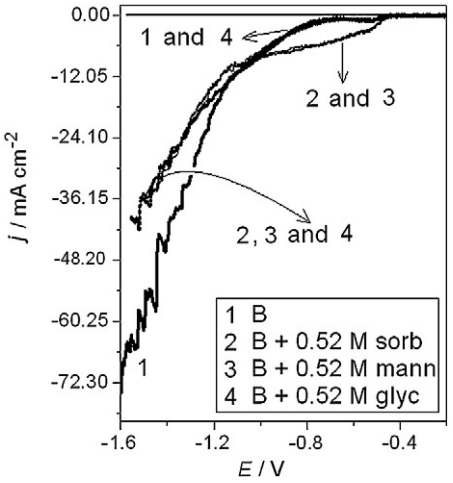

Fig. 2. Voltammetric curves of solutions, B (1.10 M Na_2SO_4, 0.26 M H_3BO_3), B + 0.52 M sorbitol, B + 0.52 M mannitol, B + 0.52 M glycerol, all cases at pH 3.0, on Pt electrode, $\upsilon = 10$ mV s^{-1}.

formed, due to the hydrogen evolution reaction (HER). These complexes favored the HER on Pt only in the initial moments of the reduction process (Fig. 2). Oliveira and Carlos [18] investigated zinc electrodeposition in the presence and absence of sorbitol and glycerol and reported that HER occurred in the initial moments of reduction and that an anodic peak of hydrogen molecular oxidation was seen in the positive sweep.

In region II (Fig. 1a and b), it can be seen that the deposition current density (j_d) decreased as the sorbitol or mannitol concentration in the bath increased. For example, at −1.40 V the fall in j_d was ~31% (0.26 M) and ~43% (0.52 M) for both polyalcohols. Also, in Fig. 1a–c there is a cathodic peak p_c for the bath without polyalcohol or baths containing 0.26 M and 0.52 M glycerol, which disappears in the presence of the boric–sorbitol (BSC) or boric–mannitol (BMC) complexes. The lower values of j_d in baths containing sorbitol or mannitol were due to adsorption of the BSC or BMC on the electrodeposit and also inhibition of reduction due to the greater molecular volume of BSC or BMC than that of glycerol, thus the BSC or BMC limits the transport of Zn and Ni ions across the metal/solution interface.

These effects could lead to modification of the morphology of the ZnNi electrodeposit. Similar results were obtained for ZnNi [10,11] or Ni [15] electrodeposition on to a Pt substrate. It must be stressed, that during preparation of solutions it was observed that those containing these complexes were more viscous. In addition, the formation of the complex between Zn^{2+} or Ni^{2+} cations and $[BSC]^-$ or $[BMC]^-$ anions could lead to decrease in the j_d. But, ultraviolet-visible spectrophometric studies showed that there was not formation of complexes between the Zn^{2+} or Ni^{2+} and $[BSC]^-$ or $[BMC]^-$ anions [15,18].

Fig. 1c shows that there was no significant variation of j_d with glycerol concentration, in contrast to BSC or BMC. This implies that glycerol did not adsorb on the electrodeposit and the morphology of the ZnNi film was unaffected by the glycerol.

It must be stressed that there was no formation of boric–glycerol complex, since was not observed a variation in initial pH (~4.0) in the baths containing glycerol in relation to bath ZnNi1, while that for the baths containing sorbitol or mannitol the pH decreased to values below 3.0 indicating the formation of complex BSC or BMC (reaction below).

$$2\,C_6H_{14}O_6 + 1\,H_3BO_3 \rightarrow [C_6H_{14}O_6 - H_2BO_3]^- + H^+$$

In addition, the pH of the plating baths ZnNi1, ZnNi1 + glycerol and ZnNi2 + glycerol was adjusted to ~pH 3.0, inhibiting the formation of products ($[C_6H_{14}O_6\text{-}H_2BO_3]^-$ and H^+) [18].

Fig. 3a–d shows galvanostatic transients (E–t) of ZnNi electrodeposition in plating baths without polyalcohol and with 0.39 M sorbitol, or 0.39 M mannitol or 0.52 M glycerol, respectively. These polyalcohol concentrations were chosen, since it was observed, by naked eye, that they afforded better ZnNi deposits. The values of j_d of 5, 25, 50 and 75 mA cm^{-2}, for ZnNi deposition, were chosen from voltammetric deposition curves (Fig. 1a–c).

The E–t transients (Fig. 3a–d) obtained from the baths without polyalcohol (ZnNi1, Fig. 3a) or with 0.52 M glycerol (Fig. 3d) were similar, except in the initial moments of E–t transients obtained at 50 mA cm^{-2}. Besides, the transients from baths containing sorbitol (ZnNi1 + 0.39 M sorbitol, Fig. 3b) or mannitol (ZnNi1 + 0.39 M mannitol, Fig. 2c) were similar. These results corroborate the similarities observed voltammetrically between mannitol and sorbitol (Fig. 1a–c). Moreover, in the E–t transients (Fig. 3b and c) in the baths containing sorbitol or mannitol, the plateau potentials (E_{pl}) were more negative than those obtained in the baths without polyalcohol or with glycerol, at

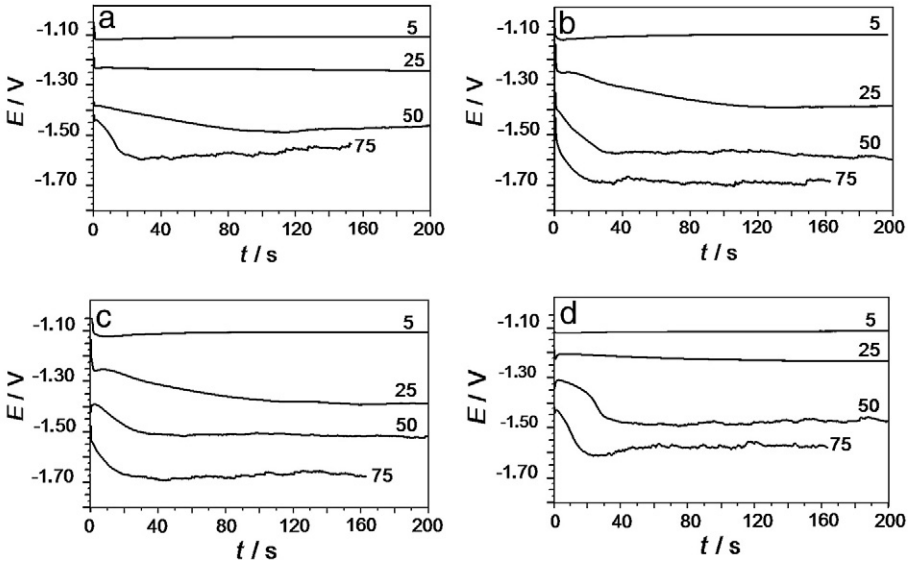

Fig. 3. Galvanostatic transient (E–t) of ZnNi deposition process, at current density of 5, 25, 50 and 75 mA cm^{-2}, from plating baths: a) ZnNi1, without polyalcohol; b) ZnNi1 + 0.39 M sorbitol; c) ZnNi1 + 0.39 M mannitol and d) ZnNi2 + 0.52 M glycerol (see Table 1).

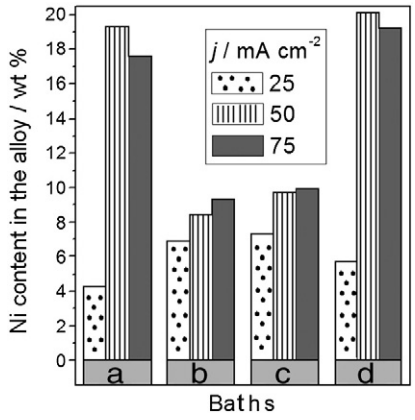

Fig. 4. (a)–(d). Ni content (wt.%) in the ZnNi alloy produced chronopotentiostatically/galvanostatically at 25, 50 and 75 mA cm^{-2}, with charge density (q) 12.21 C cm^{-2}, in baths: (a) ZnNi1, (b) ZnNi1 + 0.39 sorbitol, (c) ZnNi1 + 0.39 M mannitol and (d) ZnNi2 + 0.52 M glycerol (Table 1).

the same j_d. Thus, it may be concluded from these transients that the presence of the sorbitol or mannitol in the bath inhibited the galvanostatic deposition process, due to adsorption of the BSC or BMC on the electrodeposits surface and the large volume of these molecules.

3.2. Characterization of ZnNi electrodeposits

ZnNi deposits were laid down galvanostatically at j_d of 25, 50 and 75 mA cm^{-2}, with deposition charge density (q_d) 12.21 C cm^{-2} (thickness ~5 μm, obtained by theoretical calculation), from baths without and with 0.39 M sorbitol, 0.39 M mannitol and 0.52 M glycerol, so as to investigate the influence of the polyalcohol concentrations and j_d values on chemical composition, morphology and phase composition, by means of EDS, SEM and XRD, respectively.

3.2.1. ZnNi alloy compositional analysis by EDS

Fig. 4a–d shows the Ni content (wt.%) in the ZnNi deposits for various j_d and bath compositions. In the bath without polyalcohol, Fig. 4a, or that with 0.52 M glycerol, Fig. 4d, the Ni percentage in the electrodeposit rose, from ~5 wt.% to ~19 wt.%, as j_d changed from 25 to 50 mA cm^{-2}. At j_d 75 mA cm^{-2} there was then a small fall, ~1 wt.%, in the Ni percentage. The increase in the Ni percentage with increasing polarization has been attributed to boric acid in the plating bath [10,11,19,20].

The relative amount of Ni in the ZnNi deposit obtained from baths containing 0.39 M sorbitol, Fig. 4b, or mannitol, Fig. 4c, remained in the range of 7 wt.% to 10 wt.%, as j_d shifted in the range from 25 to 75 mA cm^{-2}. In this j_d range, the boric acid complexes, BSC or BMC favored slightly the Ni deposition. It must be stressed that such baths

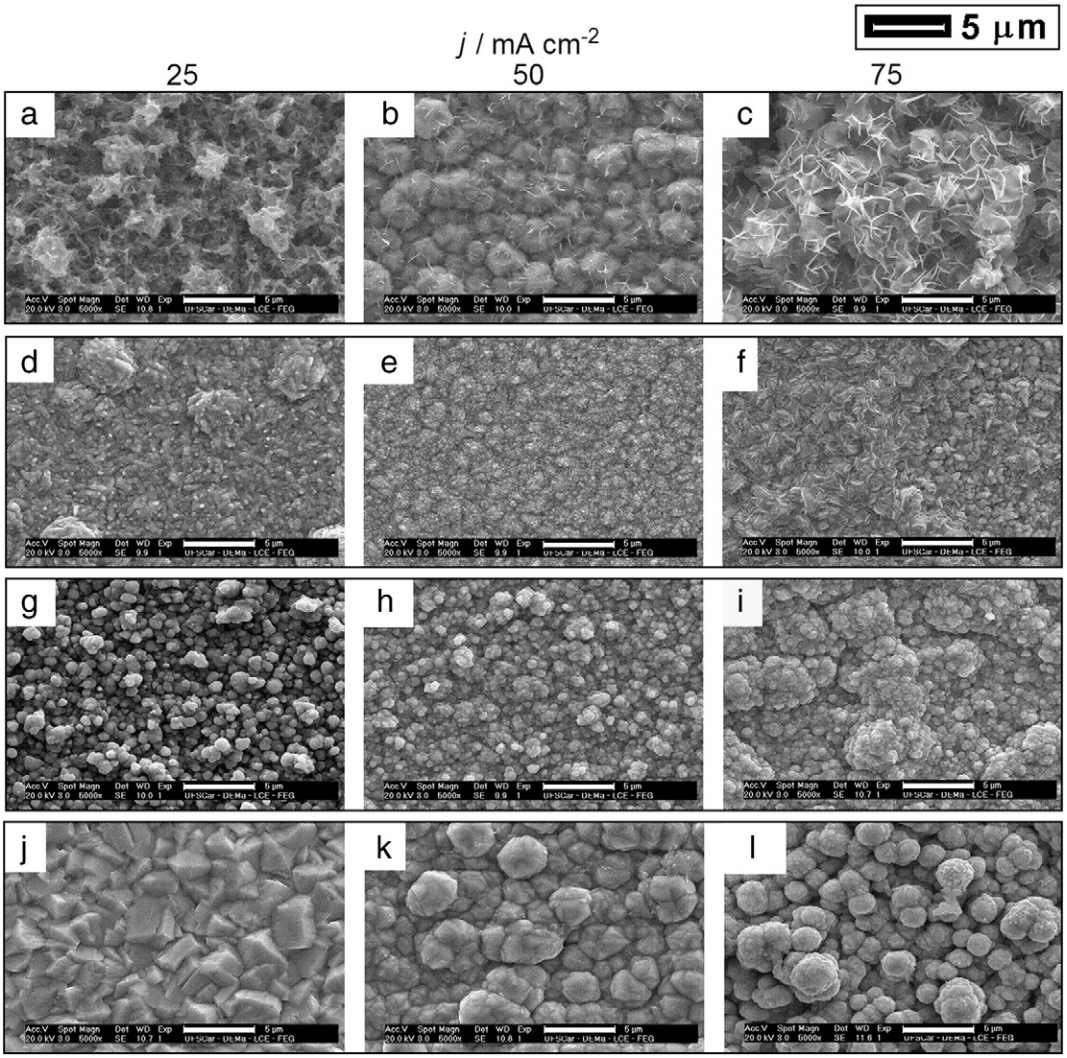

Fig. 5. SEM micrographs of ZnNi alloy films obtained chronopotentiostatically at 25, 50 and 75 mA cm^{-2}, with charge density (q) 12.21 C cm^{-2} (thickness ~5 μm), in baths: (a)–(c) ZnNi1, (d)–(f) ZnNi1 + 0.39 sorbitol, (g)–(i) ZnNi1 + 0.39 M mannitol and (j)–(m) ZnNi2 + 0.52 M glycerol (Table 1); ⊢⊣ (5 μm).

(containing BSC or BMC) have the advantage of not needing precise control of j_d. Fratesi and Roventi [21] investigated ZnNi electrodeposition from chloride baths containing NH_4Cl and observed that the content of Ni in the alloy remained approximately constant in the range of 10–50 mA cm^{-2}.

These results were similar to the previous results obtained potentiostatically on Pt substrates, in which the Ni content in the deposits obtained from solutions without polyalcohol or with various glycerol concentrations increased from ~6 wt.% to ~20 wt.% Ni, as the deposition potential (E_d) became more negative, from −1.26 V to −1.55 V, while deposits obtained from baths with various BSC or BMC concentrations showed little change in Ni content, from ~6 wt.% to ~10 wt.%, in the same potential range. Another important observation was the similarity in the Ni content, for the same range of E_d and j_d, in electrodeposits obtained with different techniques and substrates.

It has been asserted that ZnNi deposits containing between 10 wt.% and 15 wt.% Ni give the best sacrificial protection [22], or cathodic protection [23], of steel against corrosion, while others prefer the range of 15–18 wt.% Ni [24]. Thus, ZnNi deposits on to 1010 steel providing sacrificial protection can be obtained in baths with or without polyalcohols in the region of j_d studied.

The EDS analysis of the ZnNi electrodeposits led to the conclusion that the Zn and Ni codeposition was of the anomalous type.

3.2.2. ZnNi alloy morphological analysis by SEM

Fig. 5a–m shows micrographs of the ZnNi deposits. The deposits obtained from baths without polyalcohol (Fig. 5a–c) or containing glycerol (Fig. 5j–l), whose potentiodynamic deposition curves were similar, will be analyzed first. It can be seen (Fig. 5a and c) that deposits obtained from bath ZnNi1 at 25 and 75 mA cm^{-2} were less compact. At j_d 50 mA cm^{-2} (Fig. 5b), the deposit was compact with round grains of size ~3 μm, as were those obtained from bath ZnNi2 + 0.52 M glycerol (Fig. 5k and l), at j_d 50 and 75 mA cm^{-2}. In addition, in the deposit obtained from this bath at j_d 25 mA cm^{-2} (Fig. 5j), the grains had various geometric forms with well defined corners. Moreover, Fig. 5j–l shows that the deposits became less compact with increasing j_d.

The deposits obtained in ZnNi1 + 0.39 M sorbitol (Fig. 5d–f) or ZnNi1 + 0.39 M mannitol baths (Fig. 5g–i) were more compact than those discussed above, especially in the sorbitol bath, with round, more refined grains (smaller that ~1 μm) for j_d 25 and 50 mA cm^{-2} (Fig. 5d and e), while with mannitol the grains were ~1 μm. For j_d 75 mA cm^{-2} (Fig. 5f and i) the deposits were less compact.

The ZnNi deposits with better morphology were obtained at j_d 50 mA cm^{-2}, in all the baths studied. The best of these was produced in 0.39 M sorbitol, this deposit being the most refined.

These results show that the boric acid complexes, BSC or BMC, work as grain refiners, even at high j_d (75 mA cm^{-2}). Potentiodynamic curves (Fig. 1a and b) indicated that the adsorption of the boric–polyalcohol complex on the electrodeposits surface and the great size of these molecules, led to the formation of ZnNi deposits with more refined grains and to a reduction in current density (region II). The morphologies of the ZnNi electrodeposits corroborate the potentiodynamic results. The same results were observed previously in the electrodeposition of ZnNi alloy on a Pt substrate, from baths without and with these polyalcohols.

3.2.3. ZnNi alloy phase composition analysis by XRD

The observed crystallographic distances, *d(hkl)*, were compared with the expected values given in JCPDS [25].

Fig. 6a–d shows typical X-ray diffraction patterns of ZnNi deposits on 1010 steel, for j_d 50 mA cm^{-2}. The X-ray diffractograms indicate a

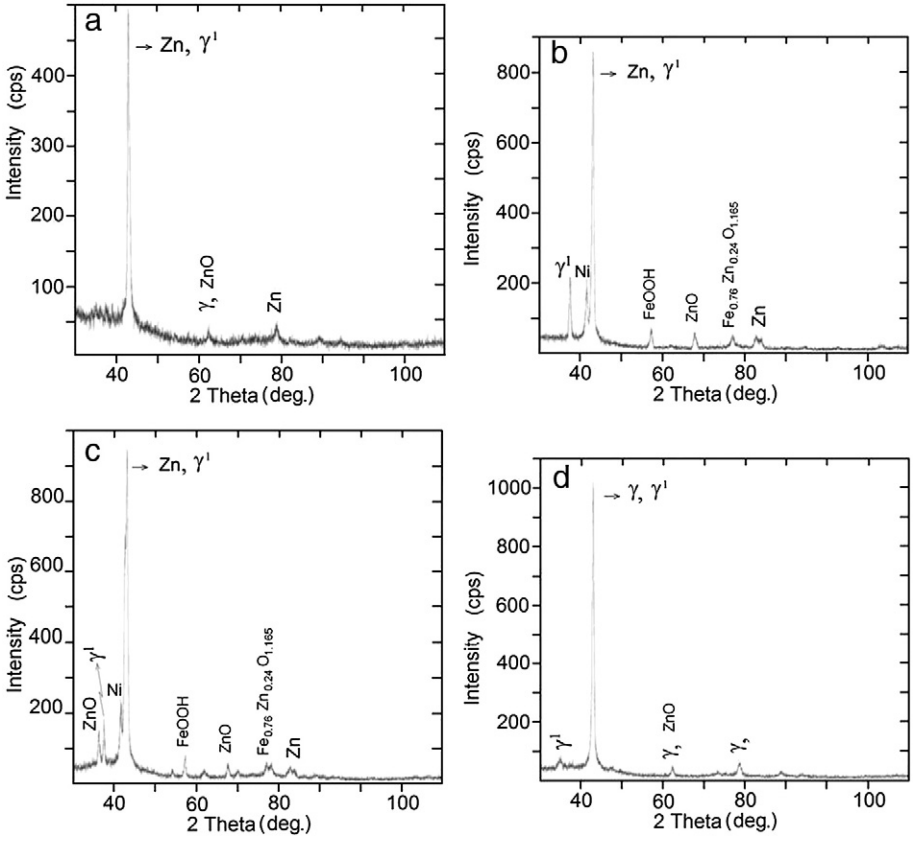

Fig. 6. X-ray diffraction patterns of ZnNi alloy obtained chronopotentiostatically at 50 mA cm^{-2}, with charge density (q) 12.21 C cm^{-2}, in baths: (a) ZnNi1, (b) ZnNi1 + 0.39 sorbitol, (c) ZnNi1 + 0.39 M mannitol and (d) ZnNi2 + 0.52 M glycerol (Table 1). Zn (PDF#06-0615), ZnO^1 (PDF#21-1486), ZnO^2 (PDF#36-1451), FeO(OH) (PDF#22-0353), ZnNi (PDF#06-0672), Zn_3Ni (PDF#47-1019), $Zn_{21}Ni_5$ (PDF#06-0653), $Zn_{22}Ni_3$, (PDF#10-0209), $Fe_{0.76}Zn_{0.24}O_{1.165}$ (PDF#48-0567).

mixture of Zn (hexagonal) and γ^1 (Zn_3Ni, orthorhombic) phases in the ZnNi deposits, to peak of greater intensity (2θ = ~43.00°) from ZnNi1, ZnNi1 + 0.39 M sorbitol and ZnNi1 + 0.39 M mannitol baths. From ZnNi2 + 0.52 M glycerol bath, to 2θ = ~43.00°, it was observed the γ ($Zn_{21}Ni_5$, cubic) and γ^1 (Zn_3Ni) phases. Considering only peak of greater intensity, it was observed different phases, Zn, γ and γ^1, in the deposits obtained at j_d 25 mA cm^{-2} from ZnNi1 + 0.39 M mannitol and ZnNi2 + 0.52 M glycerol baths, and at j_d 75 mA cm^{-2} from ZnNi1 and ZnNi2 + 0.52 M glycerol baths the γ and γ^1 phases were observed (data not shown). Thus, the presence of γ phases in the electrodeposits obtained from ZnNi2 + 0.52 M glycerol baths can to explain the bigger grain size, and Zn phases at j_d 25 mA cm^{-2} also can be favoring the formation of the grains with corners, typical of Zn electrodeposits [18]. Moreover, the X-ray diffractograms indicate a ZnO, FeOOH and $Fe_{0.76}Zn_{0.24}O_{1.165}$ phases (secondary peaks) to different baths, in different j_d. The ZnNi electrodeposits formed on steel were heterogeneous.

In addition, the X-ray diffractograms also suggested the occurrence of the δ ($Zn_{22}Ni_3$, tetragonal) in all cases and β (ZnNi, tetragonal) phases, ZnNi1 + 0.39 M sorbitol and ZnNi1 + 0.39 M mannitol baths. The formation of the δ phase by electrodeposition has been reported [6,26] and suggested by Oliveira and Carlos [10,11]. However, other authors have contested δ ($Zn_{22}Ni_3$) and β (ZnNi) phases formation by electrodeposition [22,27].

3.2.4. Study of ZnNi alloy corrosion by linear polarization

Polarization curve recorded around the open circuit potential, were used to measure R_p on 1010 steel, zinc electrodeposits and ZnNi alloy electrodeposits. The ZnNi alloy electrodeposits were produced in baths without and with 0.39 M sorbitol, 0.39 M mannitol and 0.52 M glycerol, at a current density (j_d) of 25 mA cm^{-2} and deposition charge density (q_d) of 12.21 C cm^{-2} (thickness ~5 μm), and the Zn electrodeposits in 0.55 M $ZnSO_4$ + 0.26 M H_3BO_3 + 0.52 M sorbitol [18], at j_d 50 mA cm^{-2} and the same q_d. Polarization curves of ZnNi alloy electrodeposits were also obtained at 50 mA cm^{-2} and the same q_d.

Muller et al. [28] investigated ZnNi alloy corrosion and reported that the process was controlled by activation under the conditions of study. In the cathodic branch, the main reaction was oxygen reduction, while proton reduction can be disregarded at pH >5.0. In the anodic branch, it can be assumed that the ZnNi alloy undergoes oxidation, with precipitation of zinc hydroxide on the electrodeposit due to alkalinization during the cathodic process [28]. Thus, the results obtained in this study confirm the processes described here.

Table 2 shows the mean values of corrosion potential (E_{corr}) and polarization resistance (R_p). It can be observed in Table 2 that the values of E_{corr} for ZnNi alloys (~−1.140 V to −1.028 V), irrespective of the baths, lie between the Zn E_{corr} (~−1.165 V) and the steel E_{corr} (~−0.720 V). Thus, ZnNi alloy electrodeposits generated from the various baths (Table 1) acted as sacrificial anodes.

Table 2
E_{corr} and R_p values of: 1010 steel, Zn electrodeposits and ZnNi electrodeposits produced in various ZnNi baths.

Material		E_{corr}/V	R_p/10^3 Ω cm^2
1010 Steel		−0.720	0.790
Zn electrodep. (50 mA cm^{-2})		−1.165	0.177
ZnNi1 electrodep.	25 mA cm^{-2}	−1.100	0.050
	50 mA cm^{-2}	−1.100	0.068
ZnNi1 + 0.39 M sorb. electrodep.	25 mA cm^{-2}	−1.100	0.373
	50 mA cm^{-2}	−1.095	0.525
ZnNi1 + 0.39 M man. electrodep.	25 mA cm^{-2}	−1.140	0.740
	50 mA cm^{-2}	−1.140	0.430
ZnNi2 + 0.52 M glyc. electrodep.	25 mA cm^{-2}	−1.110	0.440
	50 mA cm^{-2}	−1.028	0.545

The electrodeposits produced at 25 or 50 mA cm^{-2} from baths containing polyalcohols showed greater R_p (0.373–0.740 × 10^3 Ω cm^2) than those from bath ZnNi1 (0.050–0.177 × 10^3 Ω cm^2).

Kury et al. [23] investigated corrosion of the ZnNi alloy and reported that the corrosion resistance is more strongly affected by the structure for the deposit than by its composition. Also, Youssef et al. [29] showed that there was an increase in the corrosion resistance of Zn electrodeposits as the grain size fell. Morphological analysis of the ZnNi alloy electrodeposits (Section 3.2.2) shows that electrodeposits obtained from baths without polyalcohol were dendritic and less compact, while those obtained from baths containing BSC or BMC were more compact, with more refined grains, and from baths with glycerol, more compact. Thus, it is expected that ZnNi alloy deposited from baths contained polyalcohol is more corrosion resistance.

4. Conclusions

Potentiodynamic studies showed that during deposition there was a decrease in j_d, owing to adsorption of BSC or BMC on the electrodeposits and the large volume of these molecules, leading to a change in the deposit morphology. Galvanostatic experiments confirmed that the presence of these complexes in the baths inhibited the deposition.

SEM examination revealed that both BSC and BMC work as brighteners, even at high j_d (75 mA cm^{-2}). ZnNi deposits produced in ZnNi1 + 0.39 M sorbitol or ZnNi1 + 0.39 M mannitol baths were compact, with round, refined grains, smaller than or equal to ~1 μm, respectively, while deposits obtained from the bath of ZnNi1 were non-dendritic only at 50 mA cm^{-2} and those from the ZnNi2 + 0.52 M glycerol bath were less refined, with a grain size ~3 μm.

X-ray analysis of the ZnNi deposits produced at j_d of 50 mA cm^{-2}, in all baths, indicated that the alloys were heterogeneous, composed of a mixture of Zn and γ^1 (Zn_3Ni) phases in the ZnNi deposits from baths ZnNi1, ZnNi1 + 0.39 M sorbitol and ZnNi1 + 0.39 M mannitol. From bath ZnNi2 + 0.52 M glycerol it was observed the γ ($Zn_{21}Ni_5$) and γ^1 (Zn_3Ni) phases.

EDS analysis of the ZnNi electrodeposits led to the conclusion that the Zn and Ni codeposition was of the anomalous type. In the bath without polyalcohol or with 0.52 M glycerol, the percentage of Ni in the alloy rose from ~5 wt.% to ~19 wt.% as the j_d changed from 25 to 50 mA cm^{-2}. In baths containing 0.39 M sorbitol or mannitol, the Ni content remained in the range of 7 wt.%–10 wt.%, as j_d shifted from 25 to 75 mA cm^{-2}.

Thus, ZnNi deposits providing sacrificial protection can be produced on 1010 steel in baths with or without polyalcohol, in the region of j_d studied.

Chemical composition and phase composition results of the ZnNi alloys obtained on the 1010 steel substrate were similar to those on a Pt substrate (γ and γ^1), except for the presence of Zn alloys with Pt, indicating that the substrate did not significantly influence the composition of the ZnNi electrodeposits. However, their morphologies were influenced by the substrate and/or the electrochemical techniques, since ZnNi deposits obtained galvanostatically on 1010 steel were rougher than those obtained potentiostatically on Pt.

The linear polarization method showed that the E_{corr} of ZnNi alloy electrodeposits remained between those of the Zn electrodeposits and the 1010 steel substrate, so that the ZnNi deposits acted as sacrificial anodes. Also, the electrodeposits produced from baths containing polyalcohols showed bigger polarization resistance (R_p) than those from the ZnNi1 bath (without polyalcohols).

Acknowledgments

Financial support from the Brazilian agencies the CNPq and FAPESP are gratefully acknowledged.

References

[1] M. Pushpavanam, Bull. Electrochem. 16 (2000) 559.
[2] H. Kim, B.N. Popov, K.S. Chen, J. Electrochem. Soc. 150 (2003) C81.
[3] A. Brenner, Eletrodeposition of alloys, vol. 2, Academic Press, New York, 1963.
[4] D.H. Coleman, B.N. Popov, R.E. White, J. Appl. Electrochem. 28 (1998) 889.
[5] M. Ramasubramanian, B.N. Popov, R.E. White, J. Electrochem. Soc. 145 (1998) 1907.
[6] I. Rodriguez-Torres, G. Valentin, F. Lapicque, J. Appl. Electrochem. 29 (1999) 1035.
[7] C. Karwas, T. Hepel, J. Electrochem. Soc. 138 (1989) 1672.
[8] G. Sheela, M. Pushpavanam, S. Pushpavanam, Int. J. Hydrogen Energy 27 (2002) 627.
[9] M.L.A.D. Mertens, Tratam Superf 142 (2007) 42.
[10] E.M. Oliveira, I.A. Carlos, J. Appl. Electrochem. 39 (2009) 1313.
[11] E.M. Oliveira, I.A. Carlos, J. Appl. Electrochem. 39 (2009) 1849.
[12] S. Wolynec, Técnicas Eletroquímicas em Corrosão, Editora Universidade de São Paulo, SP, 2003.
[13] I.M. Kolthoff, J.J. Lingane, Polarography, Interscience, New York, 1952.
[14] J. Bassett, R.C. Denney, G.H. Jeffery, J. Mendham, Vogel's, Textbook of Inorganic Quantitative Analysis, 4th ed. Longman, New York, 1978.
[15] E.M. Oliveira, G.A. Finazzi, I.A. Carlos, Surf. Coat. Technol. 200 (2006) 5978.
[16] J. Ji, W.C. Cooper, Electrochim. Acta 41 (1996) 1549.
[17] R.C. Weast, Handbook of Chemistry and Physics, 1st ed. CRC Press, Florida, 1990.
[18] E.M. Oliveira, I.A. Carlos, J. Appl. Electrochem. 38 (2008) 1203.
[19] A. Petrauskas, L. Grincevicience, A. Cesuniene, E. Matulionis, Surf. Coat. Technol. 192 (2005) 299.
[20] M. Pushpavanam, K. Balakrishnan, J. Appl. Electrochem. 26 (1996) 283.
[21] R. Fratesi, G. Roventi, J. Appl. Electrochem. 22 (1992) 657.
[22] D.E. Hall, Plat. Surf. Finish. 70 (1983) 59.
[23] M.E. Soares, C.A.C. Souza, S.E. Kuri, Surf. Coat. Technol. 201 (2006) 2953.
[24] M. Pushpavanam, S.R. Natarajan, K. Balakrishnan, L.R. Sharma, J. Appl. Electrochem. 21 (1991) 642.
[25] Joint Committee on Powder Diffraction Standards (JCPDS), International Centre for Diffraction Data. Powder Diffraction File PDF-2. Database Set 1–49, ICDD, Pennsylvania, 2000, CD-ROM.
[26] S. Swathirajan, J. Electrochem. Soc. 133 (1986) 671.
[27] P.L. Cavallotti, L. Nobili, A. Vicenzo, Electrochim. Acta 50 (2005) 4557.
[28] C. Muller, M. Sarret, E. Garcia, Corros. Sci. 47 (2005) 307.
[29] Kh.M.S. Youssef, C.C. Koch, P.S. Fedkiw, Corros. Sci. 46 (2004) 51.